Wind and Structures, Vol. 15, No. 6 (2012) 531-553
DOI: http://dx.doi.org/10.12989/was.2012.15.6.531

Effect of a through-building gap on wind-induced loading and dynamic responses of a tall building

Alex P. To[1], K.M. Lam*[2], S.Y. Wong[2] and Z.N. Xie[3]

[1]Ove Arup & Partners Hong Kong Ltd, 5/F, Festival Walk, Tat Chee Avenue, Kowloon Tong, Hong Kong
[2]Department of Civil Engineering, The University of Hong Kong, Pokfulam Road, Hong Kong
[3]State Key Laboratory of Subtropical Architecture Science, South China University of Technology, Guangzhou 510641, China

(Received May 3, 2011, Revised March 1, 2012, Accepted March 5, 2012)

Abstract. Many tall buildings possess through-building gaps at middle levels of the building elevation. Some of these floors are used as sky gardens, or refuge floors, through which wind can flow with limited blockage. It has been reported in the literature that through-building gaps can be effective in reducing across-wind excitation of tall buildings. This paper systematically examines the effectiveness of two configurations of a through-building gap, at the mid-height of a tall building, in reducing the wind-induced dynamic responses of the building. The two configurations differ in the pattern of through-building opening on the gap floor, one with opening through the central portion of the floor and the other with opening on the perimeter of the floor around a central core. Wind forces and moments on the building models were measured with a high-frequency force balance from which dynamic building responses were computed. The results show that both configurations of a through-building gap are effective in reducing the across-wind excitation with the one with opening around the perimeter of the floor being significantly more effective. Wind pressures were measured on the building faces with electronic pressure scanners to help understand the generation of wind excitation loading. The data suggest that the through-building gap reduces the fluctuating across-wind forces through a disturbance of the coherence and phase-alignment of vortex excitation.

Keywords: through-building opening; wind loading; wind pressure; vortex shedding; across-wind excitation

1. Introduction

Wind-induced dynamic loading and responses are important concerns in the structural design of tall buildings, especially in typhoon/hurricane prone region. Structural engineers are always looking for ways to reduce wind-induced dynamic loads on tall buildings in order to obtain a cost effective design. One common approach is to alter the dynamic properties of the structure, such as its mass, stiffness, and damping (e.g., Irwin 2009). Another approach is to reduce the actual excitation mechanism, such as across-wind vortex excitation, by hindering the spatial coherence of vortex shedding. This can be achieved by some form of tapering or modification of the building cross-section with height (e.g., Kim and Kanda 2010a,b). Architectural modifications to the building cross-section, such as guide vanes, chamfering corners, corner cuts, and venting slots, have also

* Corresponding author, Associate Professor, E-mail: kmlam@hku.hk

been found to result in some reduction of the across-wind response (e.g., Zdrakovich 1981, Kwok and Bailey 1987, Kwok 1988, Kwok *et al.* 1988, Isyumov *et al.* 1992, Miyashita *et al.* 1993, Kwok and Isyumov 1998, Tse *et al.* 2009).

In many cities, building regulations require the provision of refuge floors in very tall buildings. In Hong Kong, for instance, a refuge floor should be provided at a level above the 25th storey in a tall building, and with an additional refuge floor required for every 25 storeys above each other refuge floor (Building Codes of Hong Kong (MOE) 1996, Cheng *et al.* 2008). Through-building gaps for other uses, such as sky gardens or architectural features for aesthetic or ventilation purposes, are increasingly common in tall building designs. These open floors are usually located at an intermediate level of the building. There has been evidence that through-building gaps or slots can be effective in reducing wind-induced dynamic excitation of a tall building. Kwok (1988) tested a lumped-mass aeroelastic model of the CAARC tall building equipped with two horizontal slots and found that building responses in both along-wind and across-wind directions were reduced. The slots occupied 3.3% of the building frontal area. With the high frequency force balance (HFFB) technique, Dutton and Isyumov (1990) showed that introduction of vertical slots on the upper part of a tall building model, of an area ratio of 6.9%, resulted in a pronounced reduction in the vortex shedding induced forces and hence the across-wind dynamic deflection of the building. Similar findings were obtained in Kikitsu and Okada (1999) by introducing an open passage of area ratio of 1.5% on a dynamic tall building model. In most of these studies, the through-building opening, in the form of either horizontal or vertical slot, was provided through the central part of the building while the perimeter of the building remained continuous. It is, however, noted that an open floor in many refugee floor or sky garden designs has the through-building opening around the perimeter of the building plan on that floor (Cheng *et al.* 2008).

In this study, we examine the effectiveness of two configurations of through-building gap in reducing the wind-induced building loads and responses. The two configurations are: (1) through-building opening through the central portions of the gap floor, and (2) through-building opening around the perimeter of the floor. The latter configuration has seldom been studied. Characteristics of fluctuating wind forces and moments on the building with either configuration of through-building gap at building mid-height were investigated with the HFFB technique in the wind tunnel. The resulting wind-induced dynamic responses of the building at different reduced velocities are analyzed. To understand the mechanism of wind load generation, wind pressures were also measured on the building model surfaces with electronic pressure scanners.

2. Wind tunnel experiments

The study was carried out in the boundary layer wind tunnel of the Department of Civil Engineering at the University of Hong Kong. The dimensions of the test section are 3.0 m width and 1.8 m height. Triangular spires at the entrance of the test section, and floor roughness elements of 8 m fetch were used to simulate boundary layer wind at a scale of 1:300. We mainly carried out testing under simulated wind of the suburban terrain type, but some tests were also made with the open sea terrain. Fig. 1 shows the vertical profiles of mean wind speed and turbulence intensities measured under the two simulated wind conditions. The target mean wind speed profiles had power exponents of 0.10 and 0.18, respectively for the open sea and suburban terrains.

All generic tall building models in the study had a square plan-form of breadth B = 0.1 m and a

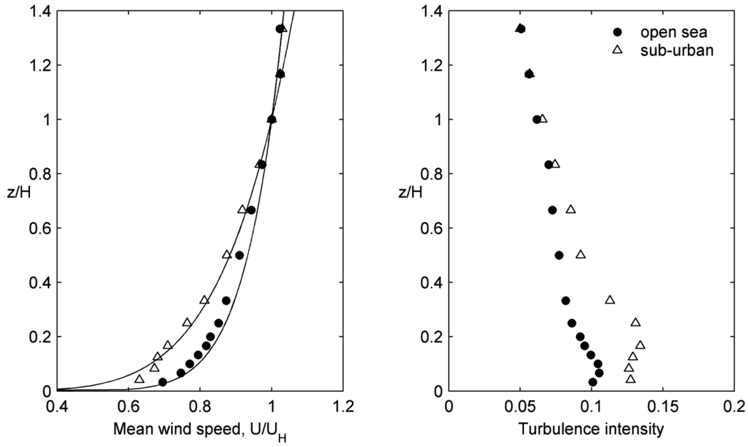

Fig. 1 Wind characteristics in wind tunnel: mean wind speed profiles (power law profiles with exponent = 0.10 for open sea and 0.18 for sub-urban terrain types); and turbulence intensity profile

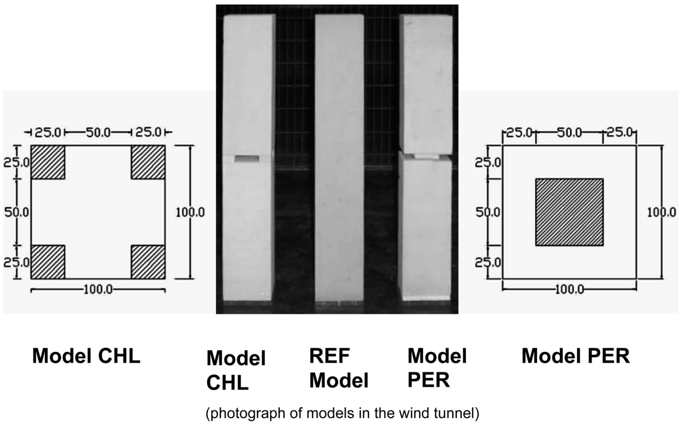

Fig. 2 Building models and configurations of through-building gap. All models are 600 mm tall. Height of gap floor is 15 mm. Dimensions in mm

height-to-breadth ratio at H/B = 6. The target geometric scale was 1:300, so the models represented full-scale buildings of height 180 m and width 30 m. The current study examined the effectiveness of two through-building gap configurations as shown in Fig. 2. The gap was always at an intermediate floor, say, a refuge floor, located at the mid-height of the building. Past studies on building openings tend to introduce slots at heights on and above the mid-building level. Slots at upper heights are expected to be more effective in reducing building responses due to greater contributions to the generalized dynamic force. In this study, our main aim was to compare the effectiveness of the two configurations of through-building opening representing a refugee floor or sky garden, thus the opening was installed at mid-building height.

In one configuration, the through-building opening was provided through the middle portion of the square cross-section of the gap floor in the form of internal flow channels. The corners of the building were thus continuous along the building height. We referred this configuration as model CHL (for "channel"). In the other configuration, model PER (for "perimeter"), there was a central core on the gap floor and the through-building opening was positioned at the perimeter of the floor section around the central core. Tests were also made on a building without a through-building gap as the reference configuration (REF model).

In model CHL or model PER alike, the through-building opening covered 75% of the floor area of the gap floor and the gap floor had a height of 15 mm in model scale or 4.5 m in full scale. At normal wind incidence to the building, the through-building opening occupied 1.25% of the frontal area of the building vertical face. This area ratio is much smaller than the values in previous studies and it may be worth investigating whether this would still lead to modifications of wind-induced building response.

Force balance models of the test tall buildings were constructed with lightweight foam materials, and fluctuating wind loads on a building model were measured with a HFFB (JR3 Inc.) mounted at the model base (Fig. 2). Time histories of the following wind load components were measured at a sampling rate of 500 Hz and over a period equivalent to more than 1 hour full-scale: base shear forces F_x, F_y, and base overturning moment, M_x, M_y along the two body axes (x-y) of the building and torsional moment M_z about the central vertical axis. Measurements were made at 15 wind incidence angles to the building with θ between 0^o and 90^o but we mainly reported results at normal wind incidences at which the largest dynamic building responses and loads occur. The orientation of the wind angle θ and directions of the body forces and moments are given in Fig. 3.

Measurements of wind pressure on the surface of a tall building model were made with a pressure model with pressure taps installed at eight levels of the building at various heights. There were eight pressure taps on each level, two on each building face. The locations of the taps are shown in Fig. 3. Each pressure tap location was denoted by the tap name and layer number (1-8). The taps are placed near the building edges to capture the negative pressures characterized by flow separation on the side faces. Fluctuating wind pressure at the tap locations was measured by electronic pressure scanners (PSI, Inc.) at a sampling rate of 200 Hz per tap. The pressure tubing for all taps was cut to the same short lengths to minimize the effect of tubing response. All pressure values were measured relative to the undisturbed ambient pressure in the wind tunnel which was measured by a pitot-static tube located above the building model.

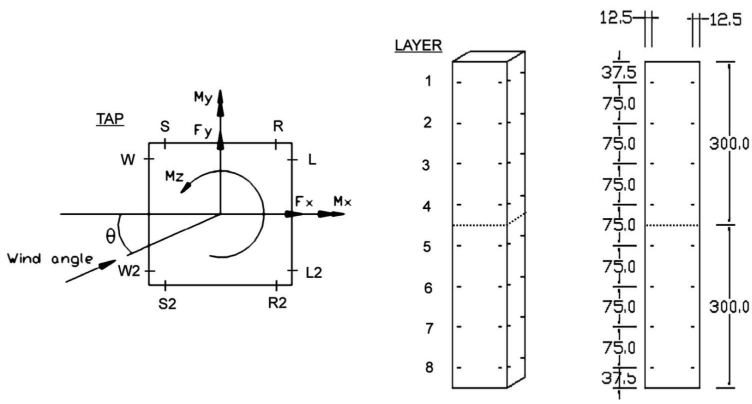

Fig. 3 Definition of wind loads and wind direction. Notation of pressure taps: windward (W), leeward (L), side (S) and rear-side (R) locations of building. Dimensions in mm. Location of gap floor shown by broken line

3. Results and discussion

3.1 Wind excitations

The overall wind forces and moments on a building model were measured by the HFFB. Fig. 4 shows the variations of mean and *r.m.s.* (root-mean-square) moment coefficient of M_y with wind angles for the three building models subject to a suburban terrain wind profile. The moment coefficients are defined in the usual way as

$$\bar{C}_{M_y} = \frac{\bar{M}_y}{\frac{1}{2}\rho\bar{U}_H^2BH^2}, \text{ and } C'_{M_y} = \frac{M_y'}{\frac{1}{2}\rho\bar{U}_H^2BH^2} \tag{1}$$

where $\bar{U}_H$ is the mean wind speed at roof height of the building, and the over-bar and the prime denote the mean and the *r.m.s.* values, respectively. The *r.m.s.* moments are the fluctuating excitations caused by wind flow around the building, and they do not include the magnification of dynamic moments as a result of wind-induced vibration of the tall building. Due to the square

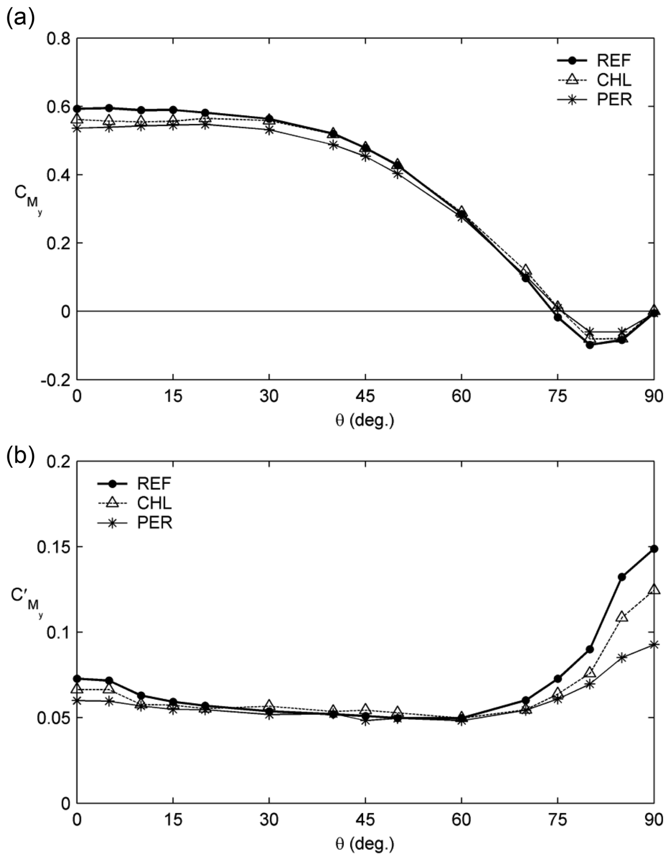

Fig. 4. Variations of *y*-direction moment coefficient with wind angle: (a) mean moment coefficients and (b) *r.m.s.* moment coefficients. Sub-urban terrain

Table 1. Across-wind moment coefficients: *r.m.s.* coefficients and peak *p.s.d.* levels

Moment coefficient	C_M'		peak $\dfrac{nS_{MM}(n)}{\left(\frac{1}{2}\rho\bar{U}_H^2BH^2\right)^2}$	
Terrain type	Sub-urban	Open sea	Sub-urban	Open sea
REF model	0.149	0.161	0.045	0.077
Model CHL	0.125	0.130	0.020	0.020
Model PER	0.093	0.093	0.009	0.015

geometry of the building, the variations of the other overturning moment coefficients ($\bar{C}_{M_x}$) are the mirror images of those curves in Fig. 4 about θ = 90° and are thus not shown. The variations of moment coefficients in Fig. 4 are typical of a square building (e.g., Lam *et al.* 2008) and the large values of C'_{M_y} at θ = 90° are caused by across-wind excitation associated with vortex shedding from the building. It is evident in Fig. 4(b) that presence of a through-building gap leads to significant reduction of this across-wind *r.m.s.* moment and there is greater reduction in model PER than in model CHL. At other wind angles away from θ = 90°, M_y has much lower *r.m.s.* values and the effects from the presence of a through-building gap are insignificant. This also applies to θ = 0° where M_y becomes the along-wind moment. For the mean wind loads in Fig. 4(a), presence of a through-building gap leads to a slight reduction in values at most wind angles but the differences are insignificant.

Similar findings are made for the mean and *r.m.s.* moments on the three building models under the open sea terrain wind profile. Table 1 lists the peak *r.m.s.* across-wind moment coefficients on buildings for the two terrain types. While higher coefficients are found for the more exposed open sea terrain, the differences become smaller on buildings with a though-building opening.

Fig. 5 shows the moment spectra in the along-wind, across-wind direction at normal incidence and at oblique incidence (θ = 45°) for the three building models under the sub-urban terrain wind profile. The power spectral densities (*p.s.d.*) are shown in the non-dimensional form of $\dfrac{nS_{MM}(n)}{\left(\frac{1}{2}\rho\bar{U}_H^2BH^2\right)^2}$ plotted against Strouhal number, $\dfrac{nB}{\bar{U}_H}$, so that a comparison of the *r.m.s.* levels of the moments can be made directly from the spectrum curves. The across-wind moment spectrum of the REF model is typical of that of a square tall building (Lam *et al.* 2008). The sharp spectral peak at $nB/\bar{U}_H \approx 0.09$ is caused by the across-wind excitation associated with shedding of vortices from the building. The frequency matches well the Strouhal number for vortex shedding from a square cylinder at value near 0.1. It is evident from Fig. 5(a) that presence of a through-building gap significantly lowers the level and sharpness of this spectral peak. It is believed that the reduction is caused by the impairment of coherent in-phase vortex excitation along the building height due to the discontinuity of a uniform building cross section at the gap floor. The reduction in model PER is found much to be more significant than that in model CHL. This is because the edges of building corners along the height of model PER are broken at the gap floor. Fig. 5(a) also shows that the building gap shifts

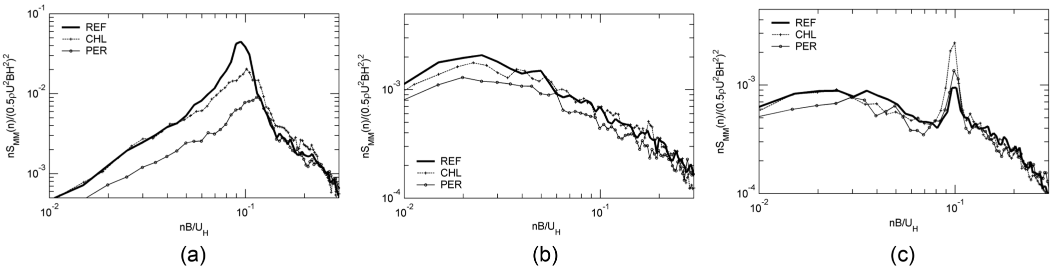

Fig. 5 Moment spectra on building models: (a) across-wind moment, (b) along-wind moment and (c) overturning moment at 45° wind incidence. Sub-urban terrain

the peak frequency slightly higher, to $nB/\overline{U}_H \approx 0.10$ and 0.11 on building models CHL and PER, respectively.

Moment spectra for the open sea terrain show similar findings and are not shown for the sake of brevity. In the across-wind moment spectra under the smoother wind flow conditions, the spectral peaks of vortex excitation are sharper, especially for the REF square building model on which the peak spectral level is much higher than that for the sub-urban terrain. A comparison of the peak spectral levels in the across-wind moment spectra is made in Table 1.

The along-wind excitation is due to turbulence buffeting with action mainly on the windward face of the building. Thus, little difference is found among those along-wind spectra for the three building models in Fig. 5(b). At the oblique wind incidence of $\theta = 45°$, the moment spectra on all three building models also have similar shapes.

Measurement results of torsional moments, M_z, on the building models in the sub-urban terrain are shown in Fig. 6 for the mean and *r.m.s.* torsion coefficients. The torsion coefficients are defined as

$$C_{M_z} = \frac{M_z}{\frac{1}{2}\rho \overline{U}_H^2 B^2 H} \tag{2}$$

Due to the square cross-sectional shape, the torsion has small values at all wind angles. Peak mean values occur at wind angles about 15° oblique to normal wind incidence cases. The largest torsion fluctuations occur at normal wind incidence where there is zero mean torsion (*Lam et al.* 2008). The presence of a through-building gap is found to lower the mean as well as the *r.m.s.* torsion at most wind angles and the reduction is higher for model PER. Wind moments and building responses in the torsional direction are not significant for all our tall building models with a square cross section. Thus, later discussion will be focused on the wind excitation and building responses in the sway direction and mostly in the across-wind direction.

3.2. Wind-induced dynamic building deflection

With the overturning moments measured on the building model, wind-induced deflections of the test tall building are estimated with the HFFB technique. Essentially, the measured moment spectra of M_x and M_y are converted to full-scale values at different full-scale wind speeds. With the assumption of linear mode shapes of vibration of the tall building, they represent the spectra of the generalized forces on the building which can be combined with the dynamic properties of the building to obtain the deflection spectra in the sway directions x and y (Tschanz 1982, Lam *et al.*

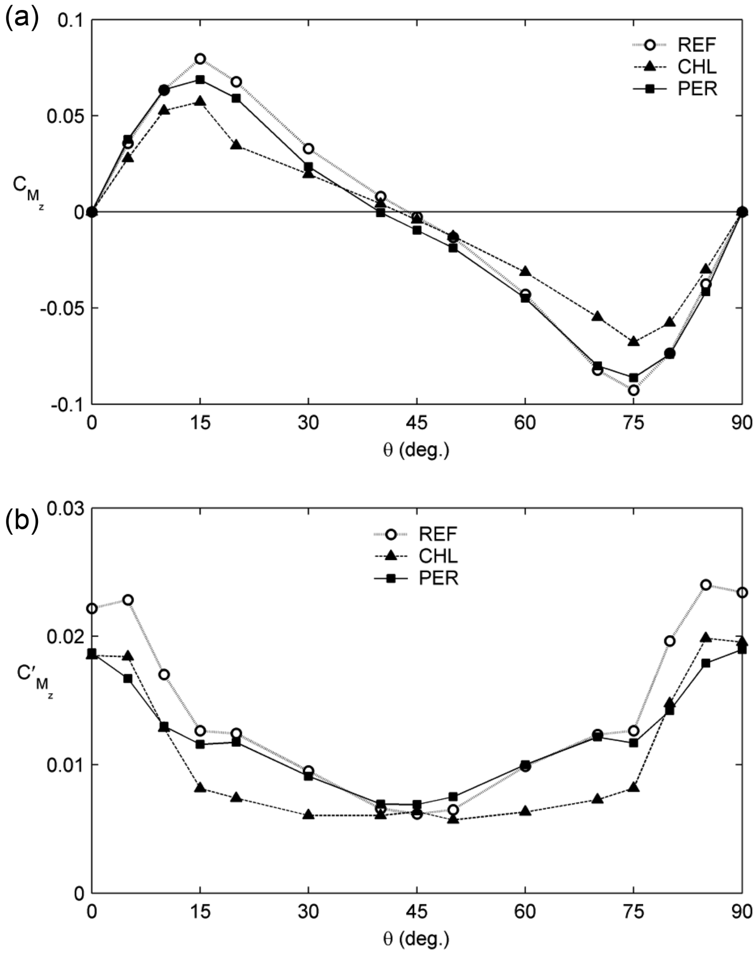

Fig. 6 Torsional moments under sub-urban terrain wind profile: (a) mean moment coefficients and (b) *r.m.s.* moment coefficients

2008, Lam and Li 2009).

Dynamic properties of the generic tall buildings in this study are borrowed from typical values for reinforced concrete residential buildings of similar dimensions. The fundamental natural frequencies in the two sway directions are assumed equal at $n_{0,x}$ = $n_{0,y}$ = 0.25 Hz. The mode shapes of these fundamental sway modes are assumed linear and uncoupled. Computation is carried out at two values of critical damping ratio for structural damping: ζ = 0.03 for strength consideration and ζ = 0.01 for serviceability assessment (Lam *et al.* 2011).

Fig. 7(a) compares the variation of top-floor *r.m.s.* deflections of the three building models in the across-wind direction under normal wind incidence for the sub-urban terrain. The data shown are y-direction accelerations at θ = 0° for 3% structural damping (ζ = 0.03). The full-scale wind speed is represented in the form of reduced velocity, $U_R = \overline{U}_H/(n_0 B)$. Fig. 7(a) shows a clear resonant across-wind response at $U_R \approx 11$ for the REF square building model. The resonant response is caused by the matching of vortex excitation frequency at this reduced velocity with n_0 of the

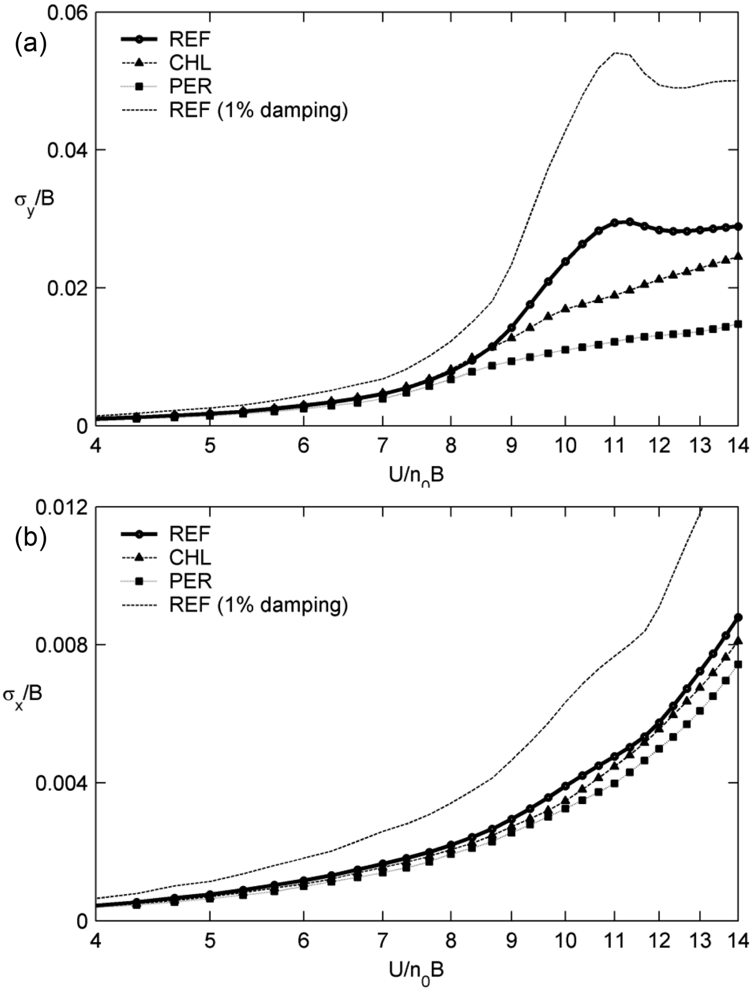

Fig. 7 Variations of wind-induced *r.m.s.* building deflections with reduced velocities, 3% structural damping, sub-urban terrain: (a) across-wind direction and (b) along-wind direction

building. The reduced velocity for resonance is the reciprocal of the value of $nB/\overline{U}_H \approx 0.09$ for the spectral peak of the across-wind moment spectra in Fig. 5(a). Wind-induced deflections of building models with a through-building gap are significantly lower than those of the REF model. This is a direct consequence of the lower levels of across-wind load fluctuations on these building models (Figs. 4(b) and 5(a)). Furthermore, the less sharp spectral peaks of vortex excitation in the across-wind spectrum for these building models (Fig. 5(a)) result in weakly noticeable resonant response behavior at reduced velocities near $U_R \approx 10$.

Between the two buildings with through-building opening, model PER experiences the smallest across-wind responses. In this model, the through-building opening along the perimeter of the section of the gap floor leads to a discontinuity of building corners along the building height. The phase alignment of vortex shedding from the building is disturbed and the overall strength of across-wind vortex excitation is thus reduced. This explains why this building model experiences the weakest across-wind responses at all reduced velocities. Wind-induced deflection responses of the three building models in the along-wind direction are shown in Fig. 7(b). At most reduced velocities, the responses are reduced from the REF model to model CHL, and then to model PER but the differences are small.

Fig. 7 also shows the wind-induced deflection response curves of the REF model for a lower structural damping of $\zeta = 0.01$. As expected, the deflections are higher but the response curve has almost the same shape as that with the higher damping. This applies to the response curves of models CHL and PER for the lower damping case which are not shown for clarity. The present study using HFFB and rigid building models cannot assess the effect of aerodynamic damping but there is evidence from previous studies employing aeroelastic model tests (Kwok 1988, Dutton and Isyumov 1990) that the building gaps result in reduction of building responses even in the presence of building motion.

Wind-induced building accelerations at the top-floor are also computed for the three building models. The acceleration response curves have very similar shapes as the deflection response curves in Fig. 7 and the same effects of through-building gap are observed. This is because in the HFFB technique, the building accelerations are dominated by the resonant component and are largely proportional to the building deflections

$$\ddot{x} = (2\pi n_0)^2 x, \; \sigma_{\ddot{x}} = (2\pi n_0)^2 \sigma_x \tag{3}$$

Fig. 8 shows, as an example, the acceleration response curves of the three building models in the across-wind direction under wind of the two terrain types. These are for a damping ratio of $\zeta = 0.01$

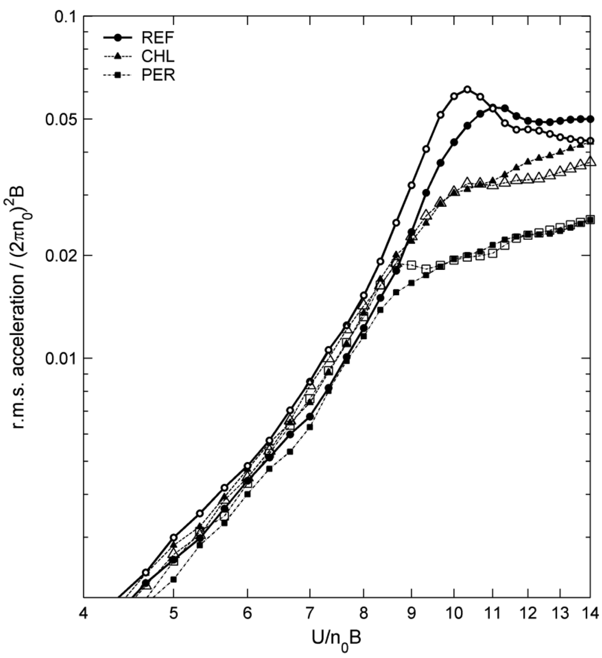

Fig. 8 Across-wind building accelerations, 1% structural damping. Closed symbols: sub-urban terrain; open symbols: open sea terrain

but as discussed earlier, the response curves at other damping values have very similar shapes. When compared to the deflection responses in Fig. 7(a), these curves for models CHL and PER show a more evident across-wind resonant response peak at $U_R \approx 10$, especially under the smoother wind flow over the open sea terrain. The shifting of spectral peak frequency of across-wind excitation to higher values for models CHL and PER observed in Fig. 5(a) is expected to cause the resonant response to occur at lower reduced velocities. This effect is not evidently observed in the deflection responses of these two building models with through-building gaps in Fig. 7(a), probably due to the largely weakened resonant responses. The more pronounced resonant acceleration responses in Fig. 8 show the expected change of occurrence of resonant response to lower reduced velocities for models CHL and PER.

In a typhoon-prone region such as Hong Kong, design values of $\overline{U}_H$ for the full-scale tall building example adopted in this dynamic response analysis have the approximate values of 42, 54 and 65 m/s, respectively at return periods of 10, 100 and 1000 years for the open sea terrain (Lam and To 2009). With n_0 = 0.25 Hz, the corresponding reduced velocities are $U_R \approx$ 5.6, 7.2 and 8.7, respectively. A comparison of effects from the two configurations of through-building opening on some realistic building response levels in the across-wind direction is made in Table 2. The table lists the *r.m.s.* top-floor building deflections for U_R = 8.7 and ζ = 0.03 and the *r.m.s.* accelerations for U_R = 5.6 and ζ = 0.01. The former design case is targeted at the structural safety criterion with a return period at 1000 years for ultimate limit state and the latter case is for serviceability with a return period at 10 years. It is evident from Table 2 that the through-building opening results in a notable reduction of building deflections in extreme winds and the percentage reduction from the REF model is about 24% for model CHL and 33% for model PER. Under serviceability wind conditions, some reductions in building accelerations are achieved from the through-building openings. There is about 10% reduction in model PER. The reductions in model CHL are very slight and there is even an increase for the sub-urban terrain. Between the two terrain types, there are always greater reductions in building responses after the installation of through-building openings under the smoother open sea terrain. This may be because vortex shedding from the REF tall building is more coherent and organized in the smoother flow and thus any impairment to vortex shedding will lead to large reductions in across-wind excitations.

If the tall buildings are more flexible, say, having a lower natural frequency n_0 = 0.20 Hz, the 1000-year return wind speed in Hong Kong will correspond to U_R = 11 under which resonant across-wind response occurs. Presence of through-building openings will then result in large reductions in the resonant deflection responses. The percentage reduction will become about 40% for model CHL and 60% for model PER.

Table 2 Across-wind responses of full-scale tall buildings under Hong Kong wind climate. Building natural frequency assumed at n_0 = 0.25 Hz

Across-wind responses	r.m.s. deflection (σ_x/B), 1000-year return, 3% damping / (fraction of REF)		r.m.s. acceleration (milli-g), 10-year return, 1% damping / (fraction of REF)	
Terrain type	Sub-urban	Open sea	Sub-urban	Open sea
REF model	0.011 / (1.00)	0.015 / (1.00)	17.6 / (1.00)	20.2 / (1.00)
Model CHL	0.011 / (0.99)	0.011 / (0.73)	19.0 / (1.08)	18.6 / (0.92)
Model PER	0.009 / (0.76)	0.010 / (0.67)	15.9 / (0.91)	16.7 / (0.82)

3.3 Wind pressure

To understand the observed effects of through-building gaps on the wind forces and moments, wind pressure data measured on building surfaces for the sub-urban terrain are analyzed. Figs. 9 and 10 show the variations of mean and *r.m.s.* pressure coefficients on the surface of the three building models at normal wind incidence ($\theta = 0°$). The pressure coefficients are computed from the division of wind pressures by $\frac{1}{2}\rho\overline{U}_H^2$. Peak values of pressure coefficients were also computed by the method of Mayne and Cook (1979) and are shown in Fig. 9. The figure shows that the distribution and levels of mean and peak pressure coefficients on the windward face (Tap W) are similar for all the three buildings. At the leeward face (Tap R), mean suction pressures (negative pressures) are measured. Their magnitudes on models CHL and PER are slightly lower than those on the REF model but they follow very similar distributions along the building height. Among the buildings, model PER experiences the lowest mean suction coefficients. It appears that the through-building gap allows more flow to pass into the wake so as to reduce the magnitude of the negative pressures. This also explains the effect of the through-building-gap in reducing slightly the mean along-wind loads on the building (Fig. 4). For the levels of pressure fluctuations, Fig. 10 shows that very similar levels of *r.m.s.* pressure coefficient, C_p', are found on the windward faces of all building models. On the leeward faces, model PER has the lowest levels of C_p' while the REF model has the highest levels of pressure fluctuations. This explains the results in Fig. 9 that among the three buildings, model PER has the smallest (absolute) peak pressure coefficients on the leeward face.

Across-wind direction wind loads are caused by wind pressure on the side faces. The side faces are under suction (negative pressure) due to flow separation at the upwind building corners. Fig. 9

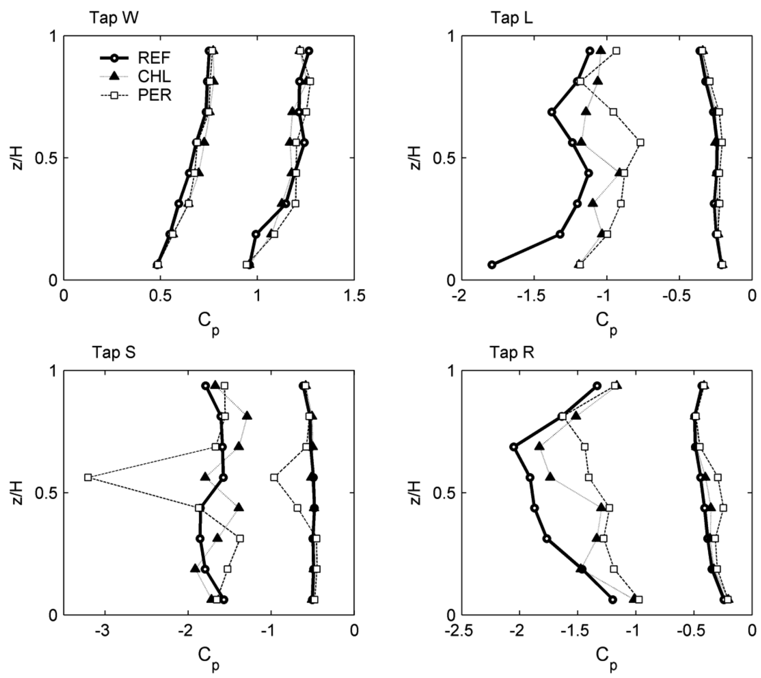

Fig. 9 Vertical distributions of mean and peak pressure coefficients (curves of higher absolute values) at four tap locations at normal incidence. Sub-urban terrain. Refer to Fig. 3 for tap locations

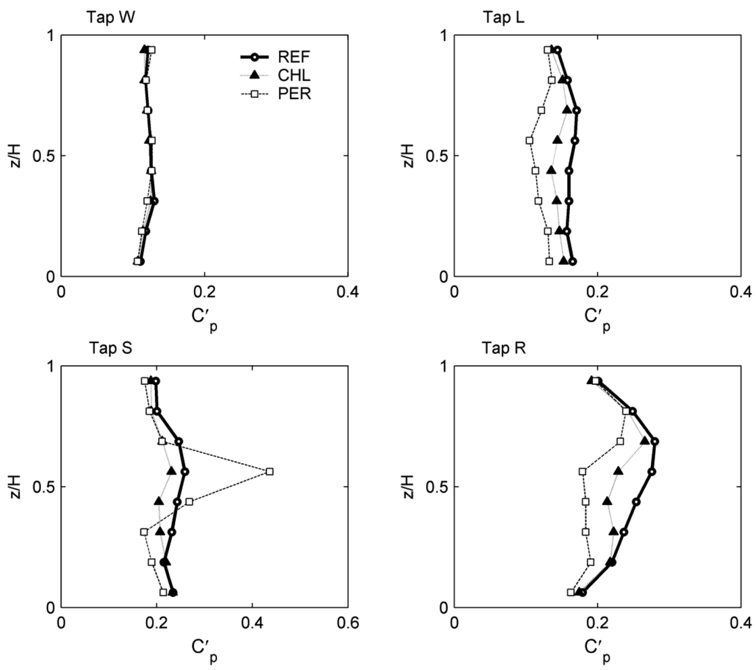

Fig. 10 Vertical distributions of *r.m.s.* pressure coefficients at four tap locations at normal incidence

shows that mean suction pressures on the side faces of models CHL and PER are generally at lower levels than those on the REF model. On model PER, very large suction pressure is found at locations just behind the separation point (Tap S, Fig. 3) and at levels near the through-building gap. This is consistent with previous wind tunnel test results of tall buildings (e.g., Kim and Kanda 2010) that high suction pressure is usually found near discontinuities in building facades. It is observed from Fig. 10 that those locations on model PER are also under very high levels of pressure fluctuation. Other than these locations, the side faces of model PER experiences the lowest levels of C_p', which have obviously lower values than that on model CHL. Both building models with a through-building gap have lower levels of pressure fluctuations on their side faces (Taps S and R) than the REF model. Thus in Fig. 9, the peak pressure coefficients on the side faces of models CHL and PER have lower magnitudes than those on the REF model.

The contribution of wind pressure at different parts of the building to the overall wind forces can be estimated by summing (or averaging) wind pressures over the areas of interest. Thus, instead of looking at pressures at individual tap locations, wind pressure signals, say at Taps W on different layers, can be summed over the building height (that is, over layers 1-8, Fig. 3) to represent the force contribution from that vertical edge zone of the building face. Fig. 11 shows the spectra of this height-averaged wind pressures for Taps W, S, R and L at normal wind incidence. The spectra are presented in the normalized form of $\dfrac{nS_{pp}(n)}{\left(\frac{1}{2}\rho\overline{U}_H^2\right)^2}$ against Strouhal Number $nB/\overline{U}_H$.

It can be observed in Fig. 11 that on the windward face, the height-averaged pressure spectra at Tap W are similar for all the three buildings, which means that the opening does not have a

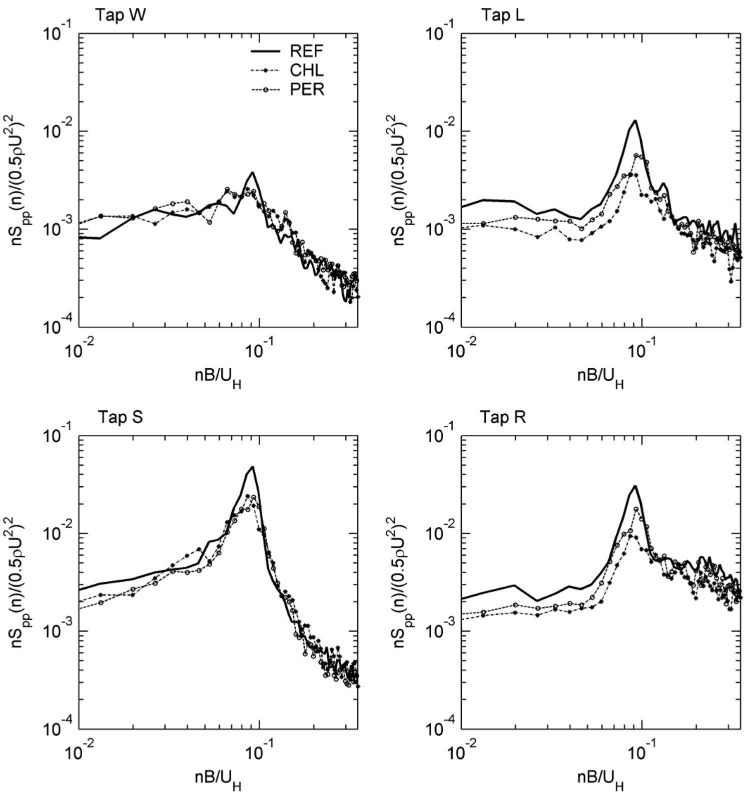

Fig. 11 Height-averaged pressure spectra at normal incidence

significant effect on the load fluctuations caused by wind pressure on the windward building face. At Tap S just behind flow separation, there are sharp peaks in the height-averaged pressure spectra at Strouhal number around 0.09, which corresponds to across-wind vortex excitation. It is observed that the spectral peaks of models CHL and PER have similar shapes, and both of them are lower than that of the REF model. This suggests that either type of through-building gaps leads to reduction in fluctuating load contribution by the wind pressure along the edge zone of the building at the vortex excitation frequency.

Tap R is on also the side face as Tap S but it is near the leeward face. The sharp spectral peaks in the height-averaged pressure spectra there have lower levels than those of Tap S. Again, the spectral peak in model CHL or PER is lower than that of the REF model. Furthermore, the spectral peak in model PER has even lower levels than model CHL, and the spectral peak around Strouhal number 0.09 is less obvious. Similar observations are made on the height-averaged pressure spectra at Tap L on the leeward faces among the three building models. The spectra there have very similar shapes as those at Tap R but the spectral levels are much lower.

We also examined the pressure spectra at individual taps and found similar observations of smoother spectral peaks in the across-wind excitation, with the presence of a through-building opening. For model PER, Fig. 10 shows very high levels of pressure fluctuations at Tap S on layers 4 and 5. Pressure spectra at these two tap locations for this building and the other two building models are shown in Fig. 12. It can be observed that the high levels of pressure fluctuations on model PER occur over all frequencies with the disappearance of the spectral peak of vortex

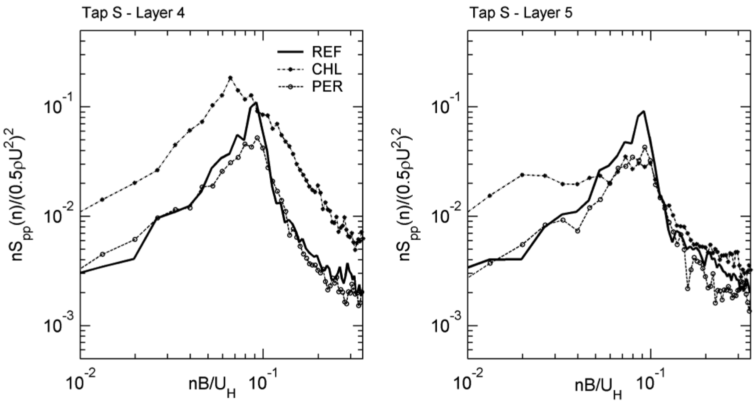

Fig. 12 Pressure spectra in edge zone of building side face (Tap S) at layers adjacent to through-building opening. Refer to Fig. 3

excitation expected at $nB/\overline{U}_H \approx 0.10$.

The results of Fig. 11 show that when the pressure fluctuations are summed (or averaged) along the building height, the resulting wind force fluctuations at frequencies of vortex excitation are reduced in the case of models CHL and PER, especially on the side faces and leeward face of the buildings. The reduction on model PER is much more pronounced than model CHL. A logical explanation is that the discontinuities of building edges on model PER disrupt the regularity and phase alignment of vortex shedding along the building height, thus reducing the integral effect of production of force fluctuations around the vortex shedding frequency. Another conjecture is that the through-building gap allows more flow to pass in the building wake through the gap floor and makes the flow around the building more three-dimensional, thus hindering the coherent production of force fluctuations from the wind pressure along the building height.

To support the first of the above two conjectures, correlation analysis is made between the wind force fluctuations contributed by wind pressures on the upper and lower parts of the buildings as divided by the gap floor. Wind pressure fluctuations at a tap location are averaged (or summed) over layers 1 to 4 and this upper-half-height-averaged pressure represents the force fluctuations contributed by wind pressures at this tap location on the upper part of the building above the building gap. The force fluctuations on the lower part of the building below the gap floor are obtained from averaging the wind pressure fluctuations over layers 5 to 8 (Fig. 3). The phase alignment, or the degree of coherence, between these two signals of force fluctuations is estimated by computing their cross correlation coefficient. Fig. 13 shows, as an example, the curves of cross correlation coefficient between the upper- and lower-half-height-averaged pressures for Tap S for the three building models. All curves exhibit some degree of periodicity with a period of time lag at $\tau\overline{U}_H/B \approx 11$ which corresponds to the Strouhal number of vortex excitation at 0.09. This suggests that wind load fluctuations due to vortex excitation are generated on both parts of the building. For all buildings, the highest value of correlation does not occur at zero time lag exactly but at a small value of τ which is about 1/10 of the quasi-period. Among the three building models, the REF model has the largest of these maximum correlation values, followed by model CHL and then model PER. The drop of the envelope peak cross correlation coefficients at increasing absolute time lag values is also faster in model CHL or PER than in the REF model. The correlation between wind load fluctuations on the two parts of the building at the most dominant frequencies is thus the

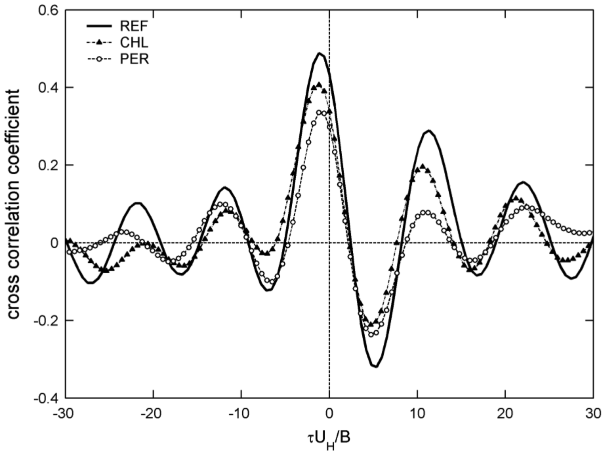

Fig. 13 Curves of cross correlation coefficients between upper- and lower-half-height-averaged pressure on edge zone of building side face (Tap S)

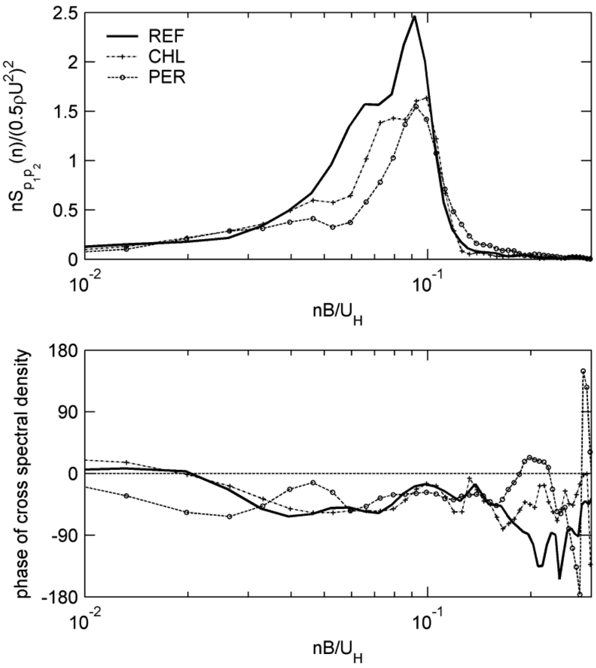

Fig. 14 Cross power spectral density (magnitude and phase) between upper- and lower-half-height-averaged pressure on Tap S

worst in model PER.

Fig. 14 shows the cross *p.s.d.* between the wind excitations at Tap S on the upper-half and lower half of the building height. In addition to the correlation information at the dominant frequency component shown by the cross correlation curves in Fig. 13, these cross spectra show the relationship at all frequency components of wind excitation. As expected, force fluctuations at the

Table 3 Cross correlation coefficients, at zero time lag, between upper- and lower-half-height-averaged pressure on the four tap locations

Location (Face)	W (windward)	S (side, edge)	R (rear-side)	L (leeward)
REF model	0.33	0.43	0.38	0.32
Model CHL	0.34	0.33	0.27	0.26
Model PER	0.33	0.32	0.29	0.30

vortex excitation frequency near $nB/\overline{U}_H \approx 0.09$ are the most correlated among all frequencies on the two building half heights of all three models. There is a second and broader peak in the cross spectra of the REF model and model CHL at a lower Strouhal number range around $nB/\overline{U}_H \approx 0.07$ to 0.08 but this is not observed on the cross spectrum of model PER. The half-height-averaged pressure excitation forces on all building models have negligible cross-power spectral levels at frequencies higher than $nB/\overline{U}_H > 0.12$. At all frequencies below this value, these excitation force fluctuations have a phase relationship near to zero.

A simple quantitative comparison on the degree of correlation of wind load fluctuations on the upper and lower parts of the building can be made from the cross correlation coefficients at zero time lag. The results for the four tap locations at normal incidence are listed in Table 3. It is noted that wind pressure fluctuations on the windward and leeward faces have a very low frequency oscillation, probably due to tunnel or instrumentation noise, and thus the signals are high-pass filtered at a cut-off frequency at $nB/\overline{U}_H \approx 0.02$ to remove the low frequency noise before computation of their cross correlation. On the windward face, similar degrees of correlation are found among the three building models. The largest differences are found on the edge zones of the side faces, where model PER shows a much lower degree of correlation.

We also studied the correlation between fluctuating wind pressures at adjacent layers along the building height. The results are consistent with the findings in Figs. 13 and 14. As an example, Fig. 15 shows the correlation curves of pressures for Tap S on the building side face. Across the through-building opening, the correlation curves between layers 4 and 5 in Fig. 15(b) show a large drop in coherence of vortex excitation for model PER. The loss of correlation for model CHL from the REF model is very much smaller. In Fig. 15(a), the correlation curves between layers 2 and 3 suggest that the effect of through-building opening in reducing the correlation of vortex excitation extends to the upper half height of model PER, though with a very slight influence. The influence is almost negligible on the lower half height of the building as shown by the pressure correlation between layers 6 and 7.

Wind-induced vibration and dynamic loading of a tall building are governed by the generalized forces and for the assumed linear mode shapes of sway-mode vibration, they are the overturning moments. Thus, it is the product of wind pressure and height of pressure tap (and the associated tributary area) that contributes to the dynamic response, with pressure fluctuations on upper parts of the buildings making larger contributions. Analysis is made on these height-weighted pressure fluctuations to investigate the contribution of different vertical parts of the building to the generalized forces or overturning moments

$$\text{contribution to } C_M = \frac{\sum_{layers} p \cdot A \cdot z}{\frac{1}{2}\rho \overline{U}_H^2 B^2 H} \tag{4}$$

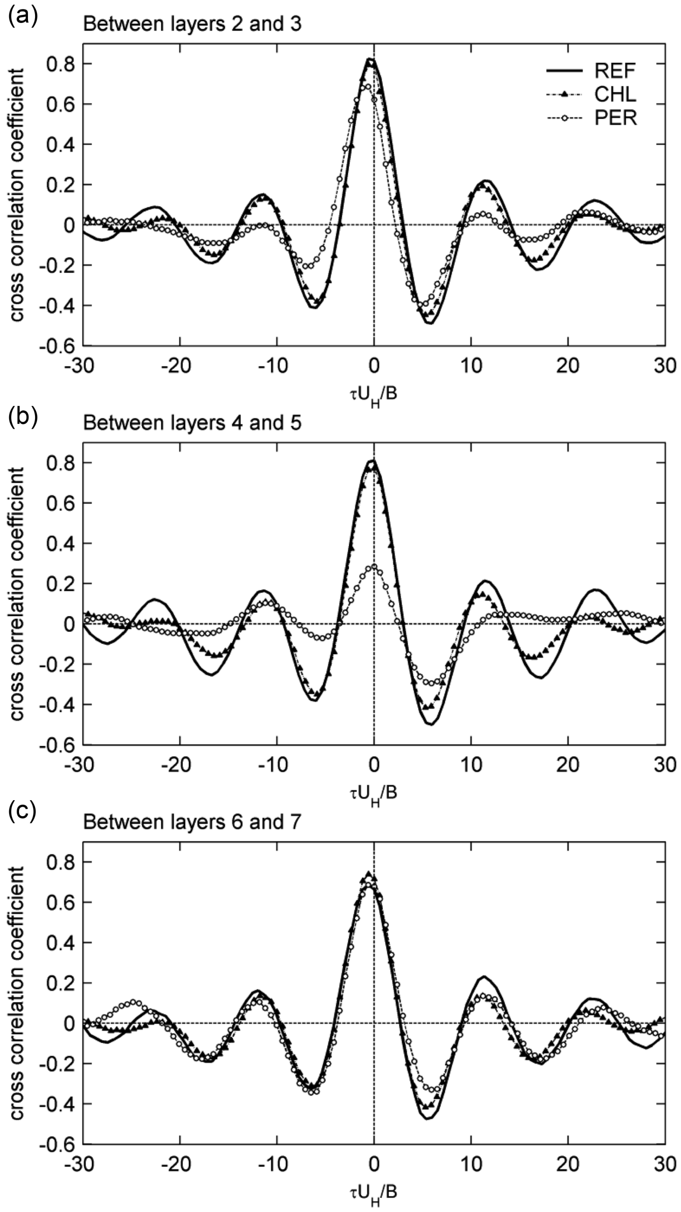

Fig. 15 Cross correlation between wind pressures at Tap S on adjacent layers: (a) layers 2 and 3 on upper half height of building, (b) layers 4 and 5 across gap floor and (c) layers 6 and 7 on lower half height of building

The summation is carried out over pressure taps on the layers (Fig. 3) of the selected vertical part of the building, A is the tributary area of pressure tap, and z is the height of tap. Fig. 16 shows the *p.s.d.* of across-wind moment coefficient contributions from the pressure at Tap S over four selected vertical parts of the building at $\theta = 0^{\circ}$. They are the upper half height of the building (layers 1 to 4), lower half height (layer 5 to 8), top quarter height of the building (layers 1 and 2), and top second quarter height (layers 3 and 4). It is observed that these *p.s.d.*'s have similar frequency distribution

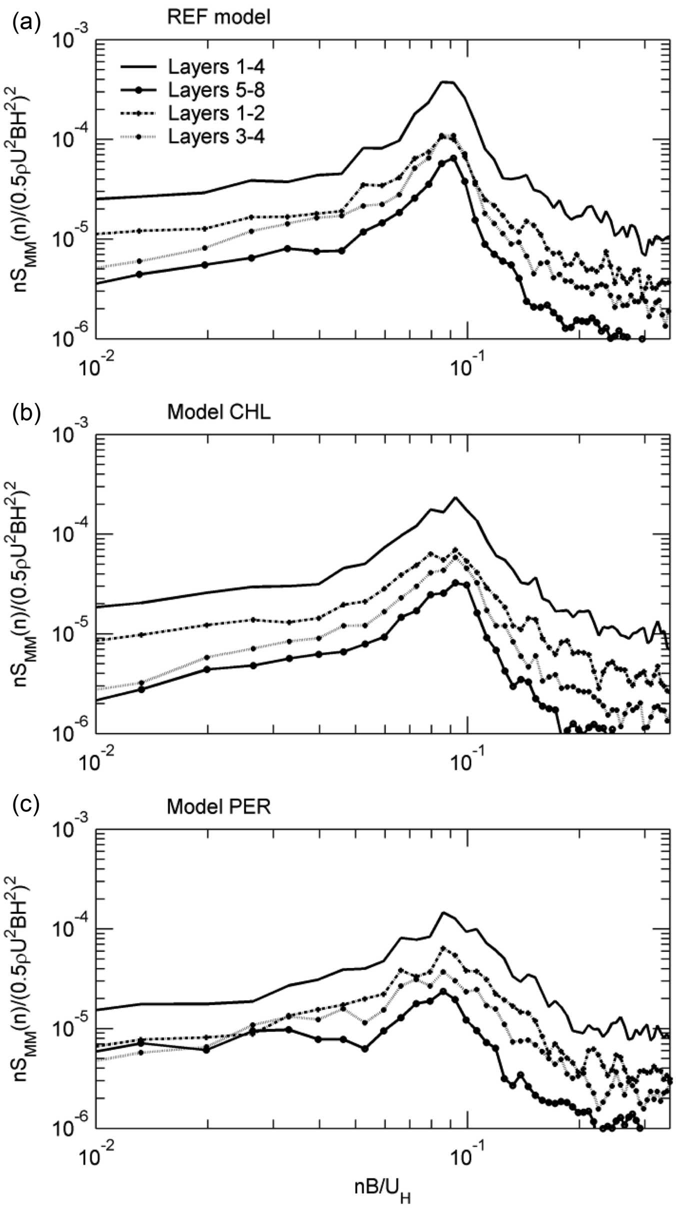

Fig. 16 Contributions of height-weighted pressure forces at Tap S over different vertical parts of building (layers, Fig. 3) to across-wind moment spectra

of energies as the height-averaged pressure spectra in Fig. 11.

Wind excitations of suction pressure from the top parts of the building contribute more to the across-wind moments. It is thus useful to study the correlation of wind excitations on the upper halves of the building models. Fig. 17 shows the cross *p.s.d.* between moment contributions from the top quarter height and top second quarter height of each building model. The results are similar to those in Fig. 14 except that for all building models, there is only one spectral peak at the vortex

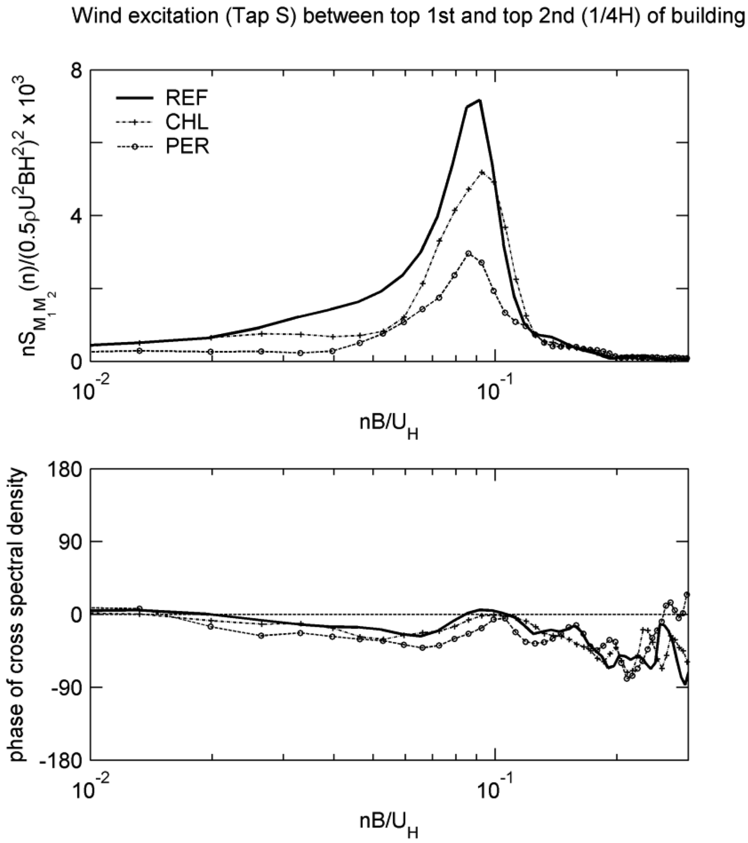

Fig. 17 Cross correlation coefficients between across-wind moment contributions from layers 1-2 and layers 3-4 (Tap S)

excitation frequency where the phase relationship is very close to zero. Similar to the observations in Fig. 15, the presence of a through-building gap at mid-height of the building is shown to result in some loss of correlation of wind excitations even over the upper half height of the building.

4. Design example

The effect of a through-building gap on wind-induced dynamic building responses has been considered in the actual design of some tall buildings. An actual example is provided here for an office building over 400 m tall in a typhoon/hurricane-prone region in Southern China near Hong Kong. The building has an approximately 50 m by 62 m rectangular plan form. The effectiveness of three through-building gap configurations in reducing wind-induced dynamic responses has been proposed and evaluated with wind tunnel testing. In all cases, a gap floor is installed at an intermediate level of the building which is the refuge floor having a storey height over twice that of a normal building storey. As shown in Fig. 18, the three configurations include (1) opening at the four corners, (2) full opening on two sides, and (3) opening around a central core. There is also a reference configuration where no refuge floor is present.

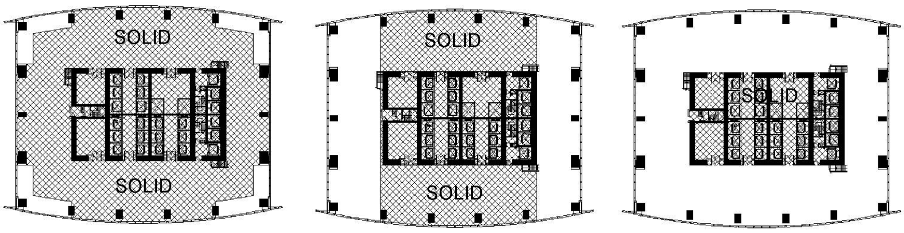

Fig. 18 Three configurations of through-building gap in design example

Table 4 Effectiveness of three through-building gap configurations in reducing wind-induced dynamic building responses in the design example

Across-wind responses:	Peak dynamic load	Peak acceleration
No through-building gap	100%	100%
(1) Opening at four corners	92%	95%
(2) Full opening on two sides	90%	87%
(3) Full opening around a central core	78%	84%

Wind-induced dynamic responses of the building in the four configurations have been assessed in the wind tunnel with the HFFB technique. The effectiveness of the three through-building gap configurations in reducing the wind-induced responses is summarized in Table 4 which shows the building responses as percentages of those of the reference building. The responses shown are the peak across-wind load at 100-year return the 10-year return peak across-wind acceleration. It is clear from Table 4 that either configuration of through-building gap is beneficial to this particular project. Configuration (3) which is similar to model PER in the parametric study results in the largest reduction in across-wind responses.

The high effectiveness of through-building opening in reducing the design dynamic wind loads and accelerations of this particular building is attributed to the low natural frequency of this very tall building at n_0 < 0.15 Hz. The reduced velocities corresponding to the 10-year and 100-year return wind speeds at the building roof height are $U_R \approx 6.6$ and 9.2, respectively.

5. Conclusions

This paper describes investigations of the effect of a through-building gap on the wind-induced dynamic responses of a tall building. The investigation was made on wind tunnel models with the HFFB measurement and analysis technique. Two gap configurations, where through-building opening is provided through the central portions of the gap floor or around the perimeter of the gap floor, are studied. Wind pressure is measured on some locations of the building faces to understand the generation of wind loads and the spectral contents and correlation of wind loads on different parts of the building surfaces.

In the absence of any through-building gap, the reference tall building model with a square planform was found to exhibit the well-reported behavior of wind-induced dynamic responses. At normal incidence, vortex shedding from the building occurs and a strong and sharp spectral peak is found in the wind pressure spectra at Strouhal number near 0.09. A high level of correlation is found between the resulting across-wind load fluctuations on the upper and lower parts of the building. These coherent vortex excitations produce strong across-wind actions and severe resonant building responses occur at reduced velocities near 11.

When a gap floor with opening around its perimeter is installed at mid-height of the building, across-wind vortex excitation is found to be impaired by the discontinuities of building edges along the building height. Wind load spectra contributed by wind pressures at the edge zones of the side faces exhibit weaker and smoother spectral peaks of vortex excitation. Compared with the reference building without a through-building gap, significantly lower degree of correlation is found between the across-wind load fluctuations on the parts of the building side face above and below the gap floor. As a result, less severe resonant across-wind responses are expected to occur. The reduction in across-wind actions is also observed on the measured data of the corresponding *r.m.s.* loading coefficients and load spectra. There are, however, insignificant modifications to the mean wind loads, as well as the along-wind actions. For the pressure coefficients on the building faces, very high mean suction and increased levels of pressure fluctuations are found on the edge zone of the side faces at levels near the gap floor. The presence of the gap floor leads to slightly lower mean suction and lower levels of pressure fluctuations on the leeward face.

In the other configuration of a through-building gap, an opening is provided through the central portion of the gap floor. The building edges thus remain continuous along the whole building height. The measurement results show less significant impairment of across-wind excitation than the through-building gap configuration with vertical building edges discontinuous at the gap floor. The evidence is in the *r.m.s.* loading coefficients and load spectra in the across-wind direction. The degree of correlation between the wind load fluctuations on the upper and lower parts of the building is only slightly reduced from the reference building model.

The effectiveness of a through-building gap in reducing the wind-induced dynamic responses of a tall building is illustrated with an actual design example. The findings show good correlation with those of the test configurations.

Acknowledgements

The last author would like to acknowledge National Natural Science Foundation of China (Grant no. 90715040) for supporting his contribution in this work. The second author would like to thank Research Grants Council of Hong Kong for partial support of this study (HKU/713507) and Mr. K.C. Chan and Mr. Ivan Li, students at the University of Hong Kong, who have assisted in some of the wind tunnel experiments.

References

Building Codes of Hong Kong (MOE) (1996), *Code of practice of the provision of means of escape in case of fire. Build*, Auth. Hong Kong, 29-33.

Cheng, C.C.K., Lam, K.M. and Demirbilek, N. (2008), "Effects of building wall arrangements on wind-induced ventilation through the refuge floor of a tall building", *J. Wind Eng. Ind. Aerod*., **96**(5), 656-664.

Dutton, R. and Isyumov, N. (1990), "Reduction of tall building motion by aerodynamic treatments", *J. Wind Eng. Ind. Aerod*., **36**(2), 739-747.
Irwin, P. (2009), "Wind engineering challenges of the new generation of super-tall buildings", *J. Wind Eng. Ind. Aerod*., **97**(7-8), 328-334.
Isyumov, N., Fediw, A.A., Colaco, J. and Banavalkar, P.V. (1992), "Performance of a tall building under wind action", *J. Wind Eng. Ind. Aerod*., **42**(1-3), 1053-1064.
Kikitsu, H. and Okada, H. (1999), *Open passage design of tall buildings for reducing aerodynamics response*, in: Wind Engineering into the 21st Century, (Eds. A, Larsen, G.L. Larose, F.M. and Livesey, A.A.), Balkema Publ., 667-672.
Kim, Y.C. and Kanda, J. (2010), "Characteristics of aerodynamic forces and pressures on square plan buildings with height variations", *J. Wind Eng. Ind. Aerod*., **98**(8-9), 449-465.
Kim, Y.C. and Kanda, J. (2010), "Effects of taper and set-back on wind force and wind-induced response of tall buildings", *Wind Struct*., **13**(6), 499-517.
Kwok, K.C.S. (1988), "Effect of building shape on wind-induced response of tall buildings", *J. Wind Eng. Ind. Aerod*., 28**(1-3)**, 381-390.
Kwok, K.C.S. and Bailey, P.A. (1987), "Aerodynamic devices for tall buildings and structures", *J. Eng. Mech. - ASCE*, **113**(3), 349-365.
Kwok, K.C.S. and Isyumov, N. (1998), "Aerodynamic measures to reduce the wind-induced response of buildings and structures", *Proceedings of the Structural Engineering World Wide*, San Francisco, USA, 1998, CD T179-6-CD.
Kwok, K.C.S., Wilhelm, P.A. and Wilkie, B.G. (1988), "Effect of edge configuration on wind-induced response of tall buildings", *Eng. Struct*., **10**(2), 135-140.
Lam, K.M., Leung, M.Y.H. and Zhao, J.G. (2008), "Interference effects on wind loading of a row of closely spaced tall buildings", *J. Wind Eng. Ind. Aerod*., **96**(5), 562-583.
Lam, K.M. and Li, A. (2009), "Mode shape correction for wind-induced dynamic responses of tall buildings using time-domain computation and wind tunnel tests", *J. Sound Vib*., **322**, 740-755.
Lam, K.M. and To, A.P. (2009), "Statistical analysis of extreme wind speeds in Hong Kong and Macau", *Trans. Hong Kong Inst. Eng*., **16**(1), 1-8.
Lam, K.M., Zhao, J.G. and Leung, M.Y.H. (2011), "Wind-induced loading and dynamic responses of a row of tall buildings under strong interference", *J. Wind Eng. Ind. Aerod*., **99**(5), 573-583.
Mayne, J.R. and Cook, N.J. (1979), "Acquisition, analysis and application of wind loading data", *Proceedings of the 5th Int. Conf. Wind Engineering*, Fort Collins, Pergamon Press.
Miyashita, K., Katagiri, J. and Nakamura, O. (1993), "Wind-induced response of high-rise buildings – effects of corner cuts or openings in square buildings", *J. Wind Eng. Ind. Aerod*., **50**, 319-328.
Tschanz, A. (1982), *Measurement of total dynamic loads using elastic models with high natural frequencies*, in: Workshop on Wind Tunnel Modeling Criteria and Effects, N.B.S., Gaithersburg, Mass., 1982.
Tse, K.T., Hitchcock, P.A., Kwok, K.C.S., Thepmongkorn, S. and Chan, C.M. (2009), "Economic perspectives of aerodynamic treatments of square tall buildings", *J. Wind Eng. Ind. Aerod*., **97**(9-10), 455-467.
Zdrakovich, M.M. (1981), "Review and classification of various aerodynamic and hydrodynamic means for suppressing vortex shedding", *J. Wind Eng. Ind. Aerod*., **7**(2), 145-189.

JH